# Effects of dopant segregation on lattice-diffusional creep of nanocrystalline ceramics

C. H. Hsueh and P. F. Becher
*Metals and Ceramics Division, Oak Ridge National Laboratory, Oak Ridge, Tennessee 37831, USA*
(Received 16 September 2004; published 26 January 2005)

The segregation of dopants whose electric charge is different from that of the parent ions and the formation of a space-charge layer induce a local electric field in the grain-boundary region. Depending upon the valence and local electrostatic potential, the charge carriers controlling diffusional creep can be either accumulated or depleted in this space-charge layer, and the creep rate is enhanced or diminished accordingly. A model was recently developed to examine the effects of a segregation-induced local electric field on the lattice-diffusional creep of nanocrystalline ceramics for spherical grains. However, in order to obtain closed-form solutions, the grain size was assumed to be much greater than the width of the space-charge layer in the existing analysis. This assumption can become inappropriate for nanocrystalline materials as the grain size is reduced; thus, a numerical method is used in the present study to resolve the existing equations without that assumption. Using yttria tetragonal zirconia as an example, the difference between the existing approximate closed-form solutions and the present numerical results is shown to be significant when the grain size is less than 50 nm.

DOI: 10.1103/PhysRevB.71.014115 PACS number(s): 62.25.+g, 62.20.Hg, 62.20.Fe

## I. INTRODUCTION

Superplasticity of nanocrystalline ceramics has been the subject of intensive research in the last decade,[1,2] and the deformation mechanism involves grain-boundary sliding accommodated by lattice diffusion. The lattice-diffusional creep model developed by Nabarro and Herring predicts that the strain rate has a power law dependence on the mean grain size with an exponent of −2 (Refs. 3,4). Hence, a decrease in the grain size by one order of magnitude would lead to an increase in the strain rate by two orders of magnitude, and substantially enhanced superplasticity in nanocrystalline ceramics is plausible. However, in order to suppress the grain growth and to maintain the small grain size, dopants that segregate to grain boundaries are added.[5] A local electric field is induced in the grain-boundary region because of dopant segregation and the formation of a space-charge layer. This local electric field inevitably affects the diffusion of charge carriers that control diffusional creep.[6–9] As a result, the grain-size exponent dependence of strain rate can be different from the value of −2 and a decrease in the expected creep rate of nanocrystalline ceramics may result.[6–9]

The space-charge theory was first postulated by Frenkel.[10] Because of the different formation energies of point defects in ionic crystals, the lattice discontinuities (e.g., surfaces, grain boundaries, and dislocation cores) may carry an electric charge resulting from the presence of excess ions of one sign, and this charge is compensated by a space-charge layer of the opposite sign adjacent to these lattice discontinuities. An electrostatic potential difference between the lattice discontinuities and the bulk exists in the presence of the space-charge layer which, in turn, induces the segregation of charged dopants. For example, $Ca^{2+}$ segregation in $CaCl_2$-doped-NaCl,[11] $Al^{3+}$ segregation in $Al_2O_3$-doped-MgO,[11] $Zr^{4+}$ segregation in $ZrO_2$-doped-$Al_2O_3$,[7] $Y^{3+}$ segregation in $Y_2O_3$-doped-$Al_2O_3$,[12] and $Y^{3+}$ segregation in yttria tetragonal zirconia (YTZP),[8,9,12] as well as segregation of divalent to pentavalent cationic dopants[13] in 12Ce-TZP and 2Y-TZP have been documented. Analyses of the charge distribution in the space-charge layer are complex even for pure ionic crystals. The relation between the electrostatic potential and the charge density is governed by Poisson's equation, and the charge density is a function of both the formation energies of point defects (e.g., anion and cation vacancies) and the electrostatic potential.[10,14–17] The solution for the charge distribution is subject to the conditions of electrical neutrality in the crystal and the minimum free energy that includes formation energies of vacancies, the energy of bound vacancy pairs, and the configurational entropy. When dopants are added, dopant segregation depends not only on the electrostatic potential but also on the dipole and elastic interactions.[10,14–17] This dopant segregation affects the charge distribution and modifies the electrostatic potential; thus, the complexity of the problem can be envisioned.

In order to study how dopant segregation affects lattice-diffusional creep, a simplified model was developed by Jamnik and Raj.[6] First, the defect species were differentiated between the one that accumulates in the space-charge layer to produce the local electrostatic potential and the one that controls lattice diffusion. Second, lattice diffusion was treated as one-dimensional diffusion between two parallel space-charge layers separated by a distance equivalent to the grain size. In this case, depending upon the valence and local electrostatic potential, the charge carriers controlling diffusional creep can be either accumulated or depleted in the space-charge region, and the creep rate is enhanced or diminished accordingly. For the enhanced case, the increase in strain rate was found to be quite limited. However, for the diminished case, the resistance was found to increase exponentially and the grain-size exponent dependence of the strain rate could change from −2 to −1 (Ref. 6). Jamnik and Raj's model was subsequently expanded by Gómez-García *et al.* by considering a three-dimensional geometry—i.e., a spherical grain.[9] However, in order to obtain closed-form solutions, the assumption was made that the grain size is much greater than the width of the space-charge layer. While the width of the space-charge layer is related to Debye attenuation length, it has been suggested that this width ranges

 ©2005 The American Physical Society

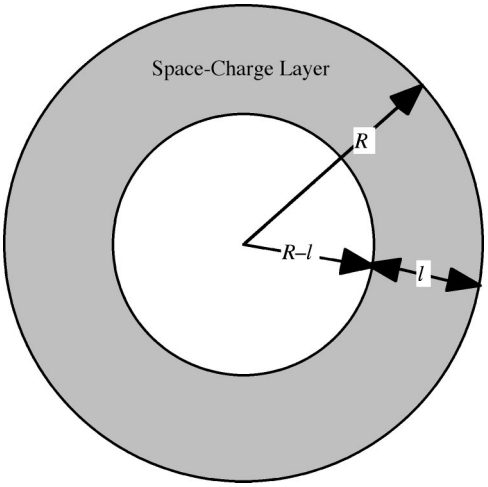


FIG. 1. Schematic showing a spherical grain with a space-charge layer.

from 2 to 10 nm by Gómez-García *et al.*[9] and from 0.4 to 3 nm by Guo and Maier.[18]

For nanocrystalline materials, the requirement that the grain size be much greater than the width of the space-charge layer would be violated. To remove this condition in the analysis and to make the solutions applicable to nanocrystalline ceramics, the purpose of the present study is to resolve the equations of Gómez-García *et al.* by using a numerical method. First, the model of Gómez-García *et al.* is summarized to provide a general background. Second, the equations of Gómez-García *et al.* are resolved using a numerical method. Finally, specific results are calculated for YTZP nanocrystalline ceramics, and the results are compared with those obtained from the approximate closed-form solutions.

## II. SUMMARY OF THE MODEL OF GÓMEZ-GARCÍA *et al.*

A spherical grain with radius $R$ is considered. The dopants segregate to the grain boundary and a space-charge layer with a width $l$ is formed in the grain-boundary region (Fig. 1). By assuming that the charge density is a constant $\rho$ within the layer $R-l \leqslant r \leqslant R$ and zero within $r=R-l$, the electrostatic potential $V$ within the grain has been derived such that[9]

$$V(r) = \frac{\rho R^2}{6\varepsilon} - \frac{\rho(R-l)^2}{2\varepsilon} + \frac{\rho(R-l)^3}{3\varepsilon R} + \frac{\rho[R^3-(R-l)^3]}{3\varepsilon_0 R} \equiv V_{\text{int}} \quad (\text{for } r \leqslant R-l), \tag{1a}$$

$$V(r) = \frac{\rho(R^2-r^2)}{6\varepsilon} + \frac{\rho(R-l)^3}{3\varepsilon}\left(\frac{1}{R}-\frac{1}{r}\right) + \frac{\rho[R^3-(R-l)^3]}{3\varepsilon_0 R} \quad (\text{for } R-l \leqslant r \leqslant R), \tag{1b}$$

where $r$ is the distance from the center of the grain, and $\varepsilon$ and $\varepsilon_0$ are the dielectric constants of the material and vacuum, respectively. The electrostatic potential in the region of $r \leqslant R-l$ given by Eq. (1a) is uniform and is denoted as $V_{\text{int}}$.

In the presence of an electrostatic potential, the concentration of the charge carriers, $c$, controlling diffusional creep is modified such that

$$c(r) = c_0 \exp\left(\frac{-ze[V(r)-V_{\text{int}}]}{kT}\right), \tag{2}$$

where $c_0$ is the concentration in the region without segregation (i.e., $r \leqslant R-l$), $z$ is the valence of the charge carrier, $e$ is the electron charge, $k$ is the Boltzmann constant (=8.6178 $\times 10^{-5}$ eV K$^{-1}$), and $T$ is the temperature.

In the absence of an electrostatic potential, the constitutive equation for creep by grain-boundary sliding accommodated by lattice diffusion is[3,4]

$$\dot{\varepsilon} = A\frac{Gb}{kT}\left(\frac{\sigma}{G}\right)^2\left(\frac{b}{d}\right)^2 D, \tag{3}$$

where $\dot{\varepsilon}$ is the creep rate, $A$ is an empirical constant, $G$ is the shear modulus, $\sigma$ is the uniaxial applied stress, $b$ is the Burgers vector, $d$ is the grain size (=2$R$), and $D$ is the lattice diffusion coefficient of the charge carrier. In the presence of an electrostatic potential, the creep equation becomes[9]

$$\dot{\varepsilon} = \alpha A\frac{Gb}{kT}\left(\frac{\sigma}{G}\right)^2\left(\frac{b}{d}\right)^2 D, \tag{4}$$

where $\alpha$ is a factor that accounts for the concentration distribution of the charge carriers and is given by

$$\alpha = \frac{R^2}{2\int_0^R \frac{c_0}{c(r)} r\,dr}. \tag{5}$$

Because $V(r)$ given by Eq. (1b) is nonuniform, a closed-form solution for $\alpha$ is unattainable when Eq. (1b) is substituted into Eqs. (2) and (5). In order to obtain closed-form solutions, two simplifications were made by Gómez-García *et al.*: (i) the grain radius was assumed to be much greater than the width of the space-charge layer—i.e., $R \gg l$—and (ii) the distribution of electrostatic potential within the layer was ignored and a mean value $\langle V \rangle$ was used. Using the above simplifications, the electrostatic potential at $r=R$—i.e., $V(R)$—and the mean electrostatic potential within the layer, $\langle V \rangle$, are[9]

$$V(R) = \frac{\rho R l}{\varepsilon_0}, \tag{6a}$$

$$\langle V \rangle = V_{\text{int}} - \frac{\rho R^2}{6\varepsilon}\left(\frac{l}{R}\right)^2. \tag{6b}$$

The parameter $V(R)$ is meaningful because it is the electrostatic potential at the grain boundary and is a measurable quantity.[9,19] A constant value of $V(R)$ is considered by Gómez-García *et al.* in their analysis. Expressing $\langle V \rangle - V_{\text{int}}$ in terms of $V(R)$, it can be obtained that

$$\frac{\langle V\rangle - V_{\text{int}}}{V(R)} = -\frac{l}{6\varepsilon_r R}, \tag{7}$$

where $\varepsilon_r = \varepsilon/\varepsilon_0$ is the relative dielectric constant. Replacing $V(r)$ in Eq. (2) with $\langle V\rangle$ and combining Eqs. (2), (5), and (7) yields

$$\alpha = \frac{1}{1 + \frac{4l}{d}\left[\exp\left(\frac{-zeV(R)}{3\varepsilon_r kT}\frac{l}{d}\right) - 1\right]}. \tag{8}$$

With the solution of $\alpha$ given by Eq. (8), the creep rate equation, Eq. (4), is complete.

In the absence of a space-charge layer, the grain size exponent of the creep rate given by Eq. (3) is −2. It is of interest to examine how the space charge affects the grain size exponent $p$, which is defined as

$$p = \left(\frac{\partial \ln \dot{\varepsilon}}{\partial \ln d}\right)_{\sigma,T}. \tag{9}$$

Substitution of Eqs. (4) and (8) into Eq. (9) yields

$$p = -2 + \frac{\frac{4l}{d}\left[1 - \frac{zeV(R)}{3\varepsilon_r kT}\frac{l}{d}\right]\exp\left(\frac{-zeV(R)}{3\varepsilon_r kT}\frac{l}{d}\right) - \frac{4l}{d}}{1 + \frac{4l}{d}\left[\exp\left(\frac{-zeV(R)}{3\varepsilon_r kT}\frac{l}{d}\right) - 1\right]}. \tag{10}$$

## III. ANALYSES

The solutions of Gómez-García *et al.* are valid when $R \gg l$. However, for nanocrystalline materials, the condition that $R \gg l$ will be violated as the grain size becomes smaller. Out of this concern, the two simplifications used by Gómez-García *et al.* are removed in the present study, and numerical results are derived. Without those simplifications, $V(R)$ and $\langle V\rangle$ derived from Eq. (1b) are

$$V(R) = \frac{\rho}{3\varepsilon_0 R}[R^3 - (R-l)^3], \tag{11a}$$

$$\langle V\rangle = \frac{3}{R^3-(R-l)^3}\int_{R-l}^{R} V(r)r^2 dr = V_{\text{int}} - \frac{\rho\{R^5 - (R-l)^5 - 5(R-l)^2[R^3-(R-l)^3] + 5(R-l)^3[R^2-(R-l)^2]\}}{10\varepsilon[R^3-(R-l)^3]}. \tag{11b}$$

In this case, $[V(r) - V_{\text{int}}]/V(R)$ and $(\langle V\rangle - V_{\text{int}})/V(R)$ become

$$\frac{V(r) - V_{\text{int}}}{V(R)} = \frac{-RF(r)}{\varepsilon_r[R^3-(R-l)^3]^2}, \tag{12a}$$

$$\frac{\langle V\rangle - V_{\text{int}}}{V(R)} = \frac{-3R\{R^5 - (R-l)^5 - 5(R-l)^2[R^3-(R-l)^3] + 5(R-l)^3[R^2-(R-l)^2]\}}{10\varepsilon_r[R^3-(R-l)^3]^2}, \tag{12b}$$

where

$$F(r) = \frac{r^2}{2} + \frac{(R-l)^3}{r} - \frac{3(R-l)^2}{2}. \tag{12c}$$

While $\langle V\rangle$ is given by Eq. (11b), it is not used to derive the creep rate in the present study; instead, it is used to derive Eq. (12b) and to check the accuracy of Eq. (7). Also, it should be noted that an area integral instead of a volume integral was used by Gómez-García *et al.* to derive $\langle V\rangle$; however, in the limiting case of $R \gg l$, $\langle V\rangle$ derived from the area and volume integrals are the same.

Substituting Eqs. (2) and (12a) into Eq. (5), the exact solution for the factor $\alpha$ can be derived, such that

$$\alpha = \frac{1}{1 - \frac{2l}{R} + \left(\frac{l}{R}\right)^2 + \frac{2}{R^2}\int_{R-l}^{R} Q(r)r\,dr}, \tag{13}$$

where

$$Q(r) = \exp\left(\frac{-zReV(R)F(r)}{\varepsilon_r[R^3-(R-l)^3]kT}\right). \tag{14}$$

The integral in Eq. (13) can be solved numerically. However, the exact closed-form solution can be obtained for the special case of $R = l$ such that

$$\alpha = \frac{zeV(R)}{2\varepsilon_r kT\left[1-\exp\left(\frac{-zeV(R)}{2\varepsilon_r kT}\right)\right]} \quad (\text{for } R=l). \quad (15)$$

While Eq. (13) shows the grain-size dependence of $\alpha$, Eq. (15) shows that $\alpha$ is independent of the grain size at $R=l$ if $V(R)$ is independent of the grain size. Equation (15) also serves as a checkpoint for the accuracy of the numerical integral in Eq. (13).

Substituting Eqs. (4) and (13) into Eq. (9), it can be shown that the grain-size exponent is

$$p = -2 + \alpha\left\{-\frac{2l}{R}\left(1-\frac{l}{R}\right)+\frac{4}{R^2}\int_{R-l}^{R} Q(r)rdr - 2\left[Q(R)-1+\frac{l}{R}\right]\right\} + \frac{2\alpha zeV(R)}{\varepsilon_r R[R^3-(R-l)^3]kT} \times \int_{R-l}^{R}\left\{\frac{l(-3R^2+l^2)F(r)}{R^3-(R-l)^3} + \frac{3R(R-l)(R-l-r)}{r}\right\}Q(r)rdr, \quad (16)$$

where $F(r)$, $\alpha$, and $Q(r)$ are given by Eqs. (12c), (13), and (14), respectively, and $Q(R)$ is $Q(r)$ at $r=R$. The solution of $p$ from Eq. (16) requires numerical integration.

## IV. RESULTS

Specific results are calculated using materials properties pertinent to YTZP in order to elucidate the essential trends. In this case, the grain boundary carries a positive charge resulting from the segregation of $Y^{3+}$, and this positive charge is compensated by a negative space-charge layer of ionic defects of $Y^{3+}$ substituting for $Zr^{4+}$—i.e., $Y'_{Zr}$ (Refs. 13,18). Within the space-charge layer, the oxygen vacancies are depleted and their contribution to the charge density can be ignored.[18] The charge carrier controlling creep is $Zr^{4+}$ and $z=4$. The materials properties are $l=5$ nm, $\varepsilon_r=4.65$, and $eV(R)=-1.5$ eV.[9] Also, unless noted otherwise, $T=1200$ °C is used in the present calculation. The relative electrostatic potential $[V(r)-V_{\text{int}}]/V(R)$ within the layer is shown in Fig. 2(a) as a function of the relative position $r-(R-l)$ at different grain sizes. The simplified result of Gómez-García *et al.* $[(\langle V\rangle - V_{\text{int}})/V(R)$ given by Eq. (7)] is also included in Fig. 2(a) for comparison. The relative positions of $r-(R-l)=0$ and 5 nm correspond to the positions at $r=R-l$ and $R$, respectively. At $r=R-l$, $[V(r)-V_{\text{int}}]/V(R)=0$ and it decreases as $r$ increases. Also, at the same relative position, the difference between $V(r)$ and $V_{\text{int}}$ increases as the grain size decreases. The corresponding relative concentration of $Zr^{4+}$, $c(r)/c_0$ and $\langle c\rangle/c_0$, are shown in Fig. 2(b). At $r=R-l$, $c(r)/c_0=1$ and it decreases as $r$ increases. The charge carrier controlling diffusion, $Zr^{4+}$, is depleted in the space-charge layer. Also, at the same relative position, $Zr^{4+}$ is more depleted as the grain size decreases. In order to check the accuracy of the closed form solutions of Gómez-García *et al.* $[\langle V\rangle - V_{\text{int}}]/V(R)$ defined by Eqs. (7) and (12b) is shown in Fig. 3 as functions of the grain size $d$. The deviation between these two curves becomes significant as the grain size is decreased below 50 nm.

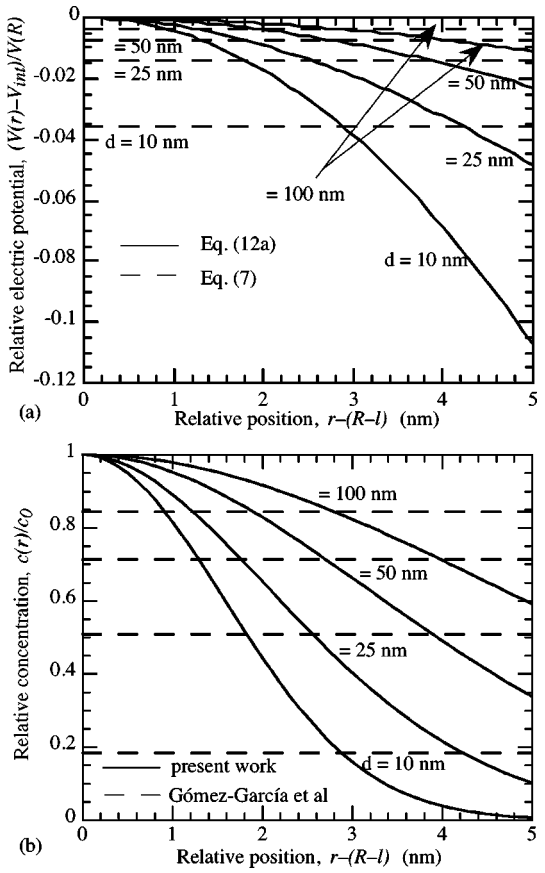


FIG. 2. (a) The relative electrostatic potential $(V(r)-V_{\text{int}})/V(R)$ and $(\langle V\rangle - V_{\text{int}})/V(R)$ and (b) the relative concentration of $Zr^{4+}$, $c(r)/c_0$ and $\langle c\rangle/c_0$, within the space-charge layer as functions of the relative position, $r-(R-l)$, at different grain sizes.

In the presence of space charge, the creep rate is modified by multiplying a factor $\alpha$. This factor is a function of both the grain size and temperature. The numerical and approximate closed-formed solutions for $\alpha$ given by Eqs. (13) and

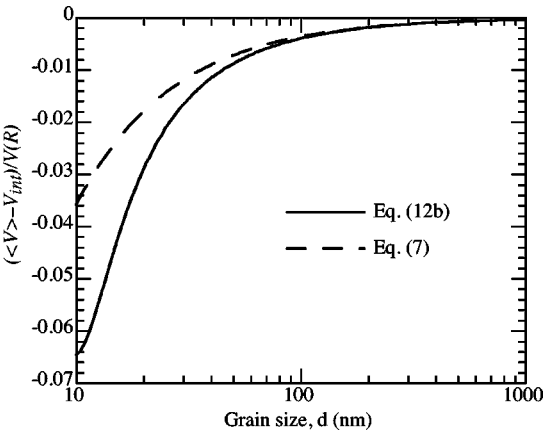


FIG. 3. The relative electrostatic potential $(\langle V\rangle - V_{\text{int}})/V(R)$ as a function of grain size showing the comparison between the present result and the result of Gómez-García *et al.*

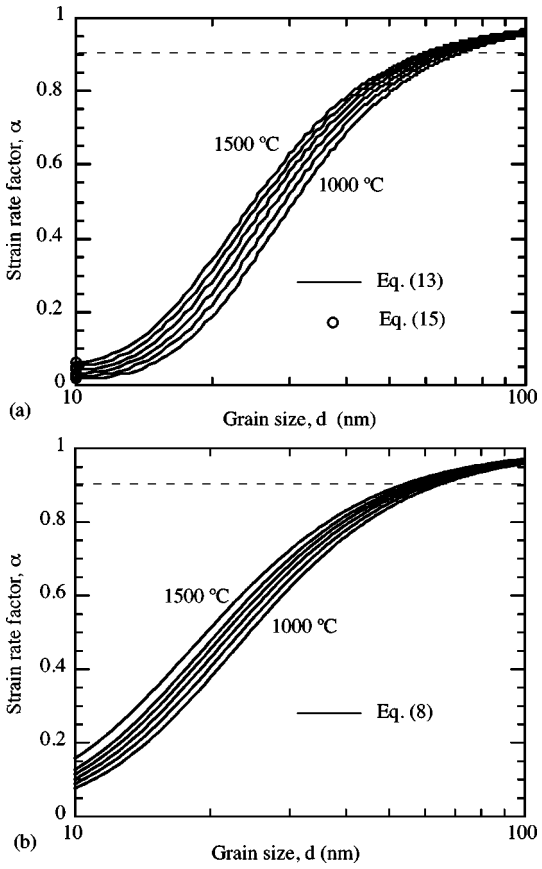


FIG. 4. The creep rate modification factor $\alpha$ as a function of grain size at temperatures 1000, 1100, 1200, 1300, 1400, and 1500 °C showing (a) the present numerical result, Eq. (13), with the present exact analytical result at $R=l$, Eq. (15), and (b) the existing approximate result, Eq. (8).

(8) as functions of grain size are shown, respectively, in Figs. 4(a) and 4(b) at different temperatures. The difference between the present numerical result and the existing approximate closed-formed solution for $\alpha$ increases with the decrease in the grain size. Also, while Fig. 4(b) shows that $\alpha$ is insensitive to the grain size only when the grain size is sufficiently large, Fig. 4(a) shows that $\alpha$ is insensitive to the grain size when the grain size is either sufficiently large or extremely small (e.g., $R$ approaches $l$). To check the accuracy of numerical integration performed on Eq. (13), the exact closed-form solution for $\alpha$ at $R=l$ given by Eq. (15) is also shown in Fig. 4(a). The excellent agreement between Eqs. (13) and (15) at $R=l$ validates the accuracy of numerical integration. It can be seen in Figs. 4(a) and 4(b) that the effects of space charge are enhanced if either the grain size or temperature is decreased. It is of interest to examine the range of temperature and grain size at which the creep rate is decreased by a certain percentage. Taking 10% (i.e., $\alpha=0.9$) as an example, the critical grain size at each temperature can be obtained from the intersections between the curves and the line at $\alpha=0.9$ in Figs. 4(a) and 4(b). This critical grain size as a function of temperature is shown in Fig. 5. By using the assumption of $R \gg l$, this critical grain size is underestimated by 5–6 nm in the temperature range of 1000–1500 °C.

The grain-size exponents $p$ given by Eqs. (10) and (16) as functions of the grain size are shown in Fig. 6, and their

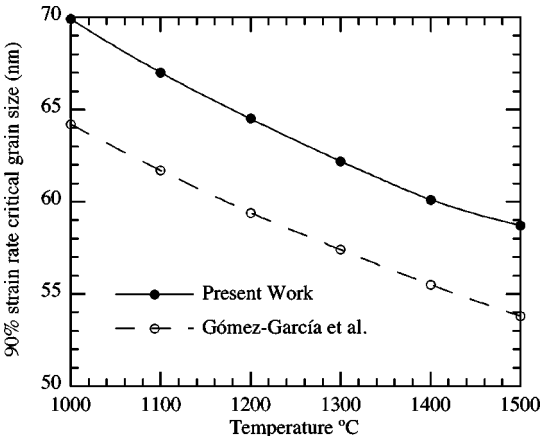


FIG. 5. The critical grain size for $\alpha=0.9$ as a function of temperature showing the comparison between the present numerical result and the analytical result of Gómez-García *et al.*

difference is evident. The exponent $p$ is $-2$ when the grain size is sufficiently large. This is consistent with experimental values[9,20,21] for submicron YTZP which are also shown in Fig. 6. Both analyses indicate that the exponent increases with decreasing grain size; however, the numerical result—i.e., Eq. (16)—shows that $p$ goes through a maximum and then rapidly decreases reaching a value of $-2$ at $R=l$. The rationale for $p=-2$ at $R=l$ is as follows. When $R=l$, Eqs. (1a) and (1b) show that $V(r)-V_{\text{int}}$ becomes independent of $R$. Because the concentration $c(r)$ is a function of $V(r)-V_{\text{int}}$ [see Eq. (2)], $c(r)$ also becomes independent of $R$ when $R=l$. As a result, $\alpha$ also no longer has a dependence on $R$ when $R=l$ [see Eq. (15)]. The slopes of the curves in Fig. 4(a) are zero at $R=l$ (i.e., at $d=2l=10$ nm). In this case, $p$ defined by Eq. (9) is not influenced by the existence of $\alpha$ in Eq. (4) when $R=l$. Hence, when the grain is fully covered by the space-charge layer, the grain-size exponent $p$ is not influenced by the existence of space charges and remains $-2$.

Although considerable effort has been dedicated to characterizing the creep of nanocrystalline ceramics, large discrepancies in the experimental data exist because the samples are not fully dense, impurities are present, or significant

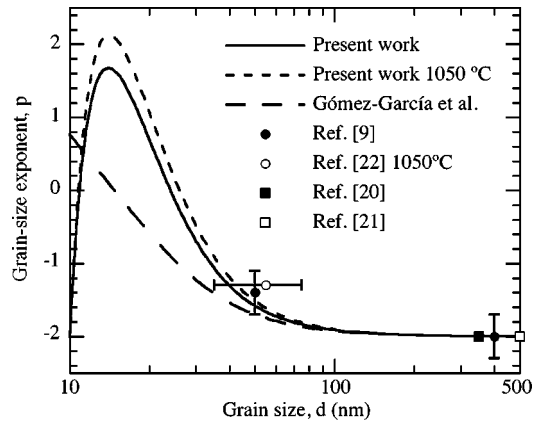


FIG. 6. The grain size exponent, $p$, as a function of grain size showing the comparison between the present numerical result and the analytical result of Gómez-García *et al.*

grain growth occurs during creep. However, recent data[9] for fully dense YTZP of 50 nm grain size at 1200 °C found a $p$ value of −1.4 that is also included in Fig. 6 for comparison. In addition, data for YTZP with 80% relative density and 35 nm initial grain size show a $p$ value of −1.3 when deforming in tension at 1050 °C; however, the grain size grows to 75 nm during the test.[22] As the data in Ref. 22 probably are influenced by grain growth and the porosity effect, the data with a grain-size error-bar are shown in Fig. 6 to reflect this grain growth. Using $T=1050$ °C, the numerical result of Eq. (16) is also shown.

## V. CONCLUDING REMARKS

Considering a spherical grain, Gómez-García *et al.* developed a model recently to examine the effects of segregation-induced space charge on lattice-diffusional creep of nanocrystalline ceramics.[9] In order to obtain closed-form solutions, they used the condition that the grain radius be much greater than the width of the space-charge layer (i.e., $R \gg l$) in solving constitutive equations. Because this condition can become invalid for nanocrystalline ceramics, the constitutive equations of Gómez-García *et al.* are resolved numerically in the present study without assuming $R \gg l$. For yttria tetragonal zirconia, the difference between the existing approximate closed-form solutions and the present numerical results is found to be significant when the grain size is less than 50 nm. However, when the width of the space-charge layer, $l$, becomes comparable to the grain radius $R$, some issues remained to be improved in the analyses. First, a uniform charge distribution in the space-charge layer is assumed in modeling. Theoretically, this charge density is a function of not only the defect formation energy but also the electrostatic potential. Because the electrostatic potential is nonuniform in the space-charge layer, a more rigorous analysis should take account of the nonuniform charge distribution. Second, $l$ is known to decrease with increasing temperature; however, it is unclear how $l$ depends on the grain size. When a larger $l$ is used in calculations, the creep resistance becomes stronger.[9] Third, Gómez-García *et al.* suggested a constant electrostatic potential at the grain boundary—i.e., $eV(R)=-1.5$ eV. In this case, the electrostatic potential in the region without segregation, $V_{\text{int}}$, described by Eq. (1a) has a finite value that is a function of the grain size. Based on Eqs. (1a) and (11a), $V_{\text{int}}$ is plotted as a function of the grain size in Fig. 7(a). It can be seen that $V_{\text{int}}$ is less than $V(R)$ and becomes closer to $V(R)$ as the grain size increases. Because the electric field in the grain-boundary region is dictated by the electrostatic potential difference across the space-charge layer, $V(R)-V_{int}$ is plotted as a function of the grain size in Fig. 7(b). It can be seen that $V(R)-V_{\text{int}}$ is ~0.16 V in the limiting case of $R \to l$ and it decreases and approaches zero as the grain size increases. Without experimental verification, it is unclear whether the result shown in Fig. 7(b) is reasonable. However, it was suggested by Guo and Maier[18] that the electrostatic potential at the grain boundary with respect to the bulk is ~0.3 V for YTZA at 500 °C. Increasing the electrostatic potential difference $V(R)-V_{\text{int}}$ used in calculations would lead to an increase in the creep resistance. Finally, the concentration of the charge carriers, $c$, controlling creep is described by Eq. (2). In this case, depletion of the charge carriers, $c$, within the space-charge layer would elevate the concentration in the region without segregation, $c_0$. Hence, a more rigorous analysis should consider conservation of charge carriers.

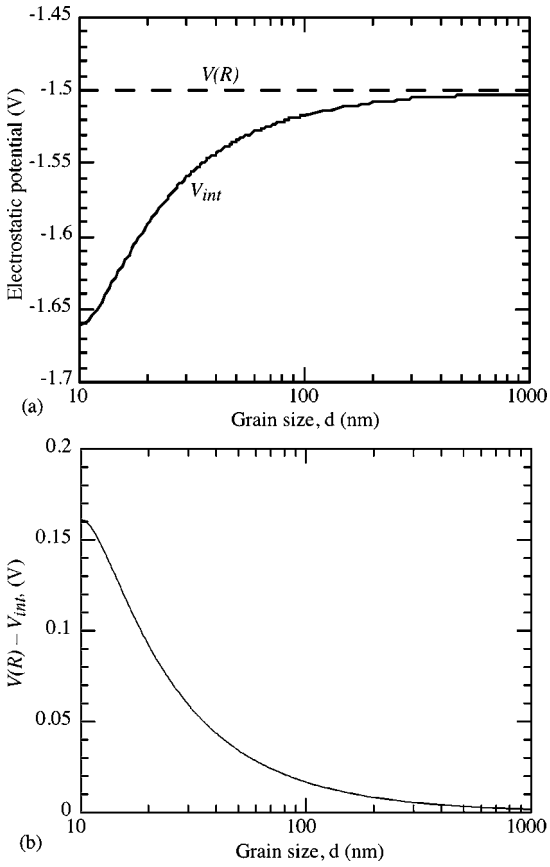


FIG. 7. (a) The electrostatic potential in the region without segregation, $V_{\text{int}}$, and (b) the electrostatic potential difference across the space-charge layer, $V(R)-V_{\text{int}}$, as functions of grain size $d$ for $V(R)=-1.5$ V.

## ACKNOWLEDGMENTS

The authors thank Dr. I. Kosacki and Dr. J. H. Schneibel for reviewing this article. This research was jointly sponsored by the U.S. Department of Energy, Division of Materials Sciences and Engineering, Office of Basic Energy Sciences, and the Heavy Vehicle Propulsion Materials Program, Office of FreedomCAR and Vehicle Technology Program under Contract no. DE-AC0500OR22725 with UT-Battelle, LLC.

[1] J. Karch, R. Birringer, and H. Gleiter, Nature (London) **330**, 556 (1987).
[2] F. Wakai, Y. Kodama, S. Sakaguchi, N. Murayama, K. Izaki, and K. Niihara, Nature (London) **344**, 421 (1990).
[3] C. Herring, J. Appl. Phys. **21**, 437 (1950).
[4] R. Raj and M. F. Ashby, Metall. Trans. **2**, 1113 (1971).
[5] I. W. Chen and L. A. Xue, J. Am. Ceram. Soc. **73**, 2585 (1990).
[6] J. Jamnik and R. Raj, J. Am. Ceram. Soc. **79**, 193 (1996).
[7] F. Wakai, T. Nagano, and T. Iga, J. Am. Ceram. Soc. **80**, 2361 (1997).
[8] M. Jiménez-Melendo, A. Domínguez-Rodríguez, and A. Bravo-León, J. Am. Ceram. Soc. **81**, 2761 (1998).
[9] D. Gómez-García, C. Lorenzo-Martín, A. Muñoz-Bernabé, and A. Domínguez-Rodríguez, Phys. Rev. B **67**, 144101 (2003).
[10] J. Frenkel, *Kinetic Theory of Liquids* (Oxford University Press, New York, 1946).
[11] W. D. Kingery, J. Am. Ceram. Soc. **57**, 1 (1974).
[12] S. Lartigue-Korinek, C. Carry, and L. Priester, J. Eur. Ceram. Soc. **22**, 1525 (2002).
[13] S. L. Hwang and I. W. Chen, J. Am. Ceram. Soc. **73**, 3269 (1990).
[14] K. Lehovec, J. Chem. Phys. **21**, 1123 (1953).
[15] J. D. Eshelby, C. W. A. Newey, P. L. Pratt, and A. B. Lidiard, Philos. Mag. **8**, 75 (1958).
[16] K. L. Kliewer and J. S. Koehler, Phys. Rev. **140**, A1226 (1965).
[17] M. F. Yan, R. M. Cannon, and H. K. Bowen, J. Appl. Phys. **54**, 764 (1983).
[18] X. Guo and J. Maier, J. Electrochem. Soc. **148**, E121 (2001).
[19] A. K. Pannikkat and R. Raj, Acta Mater. **47**, 3423 (1999).
[20] K. Morita, K. Hiraga, and Y. Sakka, Mater. Sci. Forum **357-359**, 187 (2001).
[21] G. Q. Tong, K. C. Chan, L. Lao, and Z. R. Lin, Mater. Sci. Eng., A **336**, 263 (2002).
[22] U. Betz, G. Scipione, E. Bonetti, and H. Hahn, Nanostruct. Mater. **8**, 845 (1997).